Synthesis and Characterization of New Efficient Tricarboxyterpyridyl (β-diketonato) Ruthenium(II) Sensitizers and Their Applications in Dye-Sensitized Solar Cells

Ashraful Islam,*,† Firoz A. Chowdhury,‡ Yasuo Chiba,† Ryoichi Komiya,† Nobuhiro Fuke,† Noriaki Ikeda,§ Koichi Nozaki,§ and Liyuan Han*,†

Ecological Technology Development Center, Sharp Corporation, 282-1 Hajikami, Katsuragi, Nara 639-2198, Japan, Research Institute of Innovative Technology for the Earth (RITE), 9-2 Kizugawa-dai, Kizu-Cho, Soraku-Gun, Kyoto 619-0292, Japan, and Department of Chemistry, Graduate School of Science, Osaka University, 1-16 Machikaneyama, Toyonaka, Osaka 560-0043, Japan

Received January 27, 2006. Revised Manuscript Received July 12, 2006

A new series of aryl-substituted β-diketonato-ruthenium(II)-polypyridyl sensitizers, [Ru(Htctpy)(tfpbd)(NCS){$(C_4H_9)_4N$}$_2$] (**1**), [Ru(Htctpy)(tffpbd)(NCS){$(C_4H_9)_4N$}$_2$] (**2**), and [Ru(Htctpy)(tfcpbd)(NCS){$(C_4H_9)_4N$}$_2$] (**3**), were synthesized and fully characterized by elemental analysis, UV−visible and emission spectroscopy, NMR, ATR-FTIR, cyclic voltammetric studies, and density functional theory (DFT) calculations (where tctpy = 4,4′4″-tricarboxy-2,2′:6′,2″-terpyridine, tfpbd = 4,4,4-trifluoro-1-(phenyl)-butane-1,3-dione, tffpbd = 4,4,4-trifluoro-1- (4-fluorophenyl)butane-1,3-dione, and tfcpbd = 4,4,4-trifluoro-1-(4-chlorophenyl)butane-1,3-dione). In ethanol−methanol solution, these complexes exhibit intense visible light absorption, with low-energy MLCT band maxima above 600 nm. A distinct shoulder at around 680 nm improved red-light absorptivity beyond 680 nm. Controlled shifting of the low-energy MLCT band and Ru oxidation potential can be achieved by changing the electron donor ability of the β-diketonate ligand using various aryl substituents of the β-diketonate ligand with differing electron-donating strengths. Density functional theory (DFT) calculation of complex **2** shows that the HOMO is localized on the NCS ligand and the LUMO on the tctpy ligand, which is anchored to the TiO_2 nanoparticles. The aryl-substituted β-diketonato-ruthenium(II)-polypyridyl sensitizers, when anchored to nanocrystalline TiO_2 films, achieve very efficient sensitization, with greater than 80% incident photon-to-current conversion efficiency (IPCE) in the whole visible range extending up to 950 nm. Under standard AM 1.5 irradiation (100 mW cm^{-2}) and using an electrolyte consisting of 0.6 M dimethylpropyl-imidazolium iodide, 0.05 M I_2, 0.1 M LiI, and 0.07 M *tert*-butylpyridine in acetonitrile, a solar cell containing complex **2** yielded a short-circuit photocurrent density of 19.1 mA cm^{-2}, an open-circuit photovoltage of 0.66 V, and a fill factor of 0.72, corresponding to an overall conversion efficiency of 9.1%.

Introduction

Dye-sensitized nanocrystalline TiO_2 solar cells (DSCs) have recently been under intense investigation because of their high efficiency and potential for low-cost production.[1−7] In this solar cell, a monolayer of dyes is attached to the surface of a large-bandgap nanocrystalline TiO_2 film to absorb light. Photoexcitation of the dye results in the injection of an electron into the conduction band of the oxide. The original state of the dye is subsequently restored by electron donation from a redox system, such as the iodide/triiodide couple. The dye should have suitable ground- and excited-state redox properties so that charge injection and regeneration of the dye occurs efficiently. However, it is very difficult to fulfill both requirements simultaneously when designing a dye for nanocrystalline TiO_2 solar cells that can absorb visible light of all colors. The electrochemical and photophysical properties of the dye play an important role for excited-state charge injection, dye regeneration, and charge-recombination dynamics at the semiconductor interface.[8]

The most efficient metal complex photosensitizers employed so far in DSCs are Ru(II) polypyridyl complexes because of their intense charge-transfer absorption in the whole visible range and the ease with which redox properties can be tuned by changing the donor−acceptor properties of the ligand in a controlled manner.[1,2,9−17] The two outstanding

* Corresponding author. E-mail: ashraful.islam@sharp.co.jp (A.I.); han.liyuan@sharp.co.jp (L.H.). Phone: 81-745-63-3539. Fax: 81-745-63-3306.
† Sharp Corporation.
‡ Research Institute of Innovative Technology for the Earth.
§ Osaka University.

(1) O'Regan, B.; Grätzel, M. *Nature* **1991**, *353*, 737.
(2) Nazeeruddin, Md. K.; Kay, A.; Rodicio, I.; Humphry-Baker, R.; Müller, E.; Liska. P.; Vlachopoulos, N.; Grätzel, M. *J. Am. Chem. Soc.* **1993**, *115*, 6382.
(3) Grätzel, M. *J. Photochem. Photobiol., A* **2004**, *164*, 3.
(4) Grätzel, M. *J. Photochem. Photobiol., C* **2003**, *4*, 145.
(5) Hara, K.; Sugihara, H.; Tachibana, Y.; Islam, A.; Yanagida, M.; Sayama, K.; Arakawa, H. *Langmuir* **2001**, *17*, 5992.
(6) Hagfeld, A.; Grätzel, M. *Chem. Rev.* **1995**, *95*, 49.
(7) Hagfeld, A.; Grätzel, M. *Acc. Chem. Res.* **2000**, *33*, 269.
(8) Islam, A.; Sugihara, H.; Arakawa, H. *J. Photochem. Photobiol.,* A **2003**, *158*, 131.
(9) Nazeeruddin, Md. K.; Péchy, P.; Renouard, T.; Zakeeruddin, S. M.; Humphry-Baker, R.; Comte, P.; Liska, P.; Cevey, L.; Costa, E.; Shklover, V.; Spiccia, L.; Deacon, G. B.; Bignozzi, C. A.; Grätzel, M. *J. Am. Chem. Soc.* **2001**, *123*, 1613.
(10) Nazeeruddin, Md. K.; Péchy, P.; Grätzel, M. *Chem. Commun*. **1997**, *1705*.

10.1021/cm0602141 CCC: $33.50 © 2006 American Chemical Society
Published on Web 10/06/2006

Ru(II) polypyridyl sensitizers for nanocrystalline TiO_2 solar cells so far reported are $[Ru(Hdcbpy)_2(NCS)_2\{(C_4H_9)_4N\}_2]$ and $[Ru(Htctpy)(NCS)_3\{(C_4H_9)_4N\}_3]$ (referred to as b-dye), where dcbpy is 4,4′-dicarboxy-2,2′-bipyridine and tctpy is 4,4′,4″-tricarboxy-2,2′:6′,2″-terpyridine, yielding a solar-to-electric power conversion efficiency of greater than 10% under standard AM 1.5 conditions.[2,9,18−19] The role of the monodentate thiocyanato ligand is to tune the spectral and redox properties of the sensitizers by destabilizing the metal t_{2g} orbital.

Many research groups have introduced nonchromophoric chelating ligands such as dithiocarbamates, dithiolates, and ethylenediamine donor ligands into the central metal coordination sphere instead of thiocyanate to tune sensitizer absorption properties and thus improve cell efficiency.[20−22] Recently, Sugihara et al. reported an efficient Ru(II) 4,4′-dicarboxy-2,2′-bipyridine sensitizer containing one chelating β-diketonate ligand instead of two thiocyanate ligands.[23−24] The strong σ-donating nature of the negatively charged oxygen donor atom of the β-diketonato ligand destabilizes the ground-state energy level of the dye, leading to a lower energy shift of the MLCT transitions compared to that of the thiocyanato-ruthenium(II) complex. In addition, the β-diketonato ruthenium(II) sensitizer of [Ru(4,4′,4″-tricarboxy-2,2′:6′,2″-terpyridine)(1,1,1-trifluoropentane-2,4-dionato)-(NCS)] (**C1**) with one NCS ligand shows efficient panchromatic sensitization of nanocrystalline TiO_2 solar cells.[25] The energy level can further be tuned by changing the electron donor ability of the substituents on the carbon atoms of the 1,1,1-trifluoropentane-2,4-dionato ligand to produce the desired electronic environment at the metal center.[12]

Here, we report the synthesis and characterization of terpyridine-ruthenium(II) complexes containing three different aryl-substituted β-diketonate ligands 4,4,4-trifluoro-1-(phenyl)butane-1,3-dione (tfpbd), 4,4,4-trifluoro-1-(4-fluorophenyl)butane-1,3-dione (tffpbd), and 4,4,4-trifluoro-1-(4-chlorophenyl)butane-1,3-dione (tfcpbd) and their photovoltaic performance in DSCs. The molecular structures of the three new complexes, $[Ru(Htctpy)(tfpbd)(NCS)\{(C_4H_9)_4N\}_2]$ (**1**), $[Ru(Htctpy)(tffpbd)(NCS)\{(C_4H_9)_4N\}_2]$ (**2**), and $[Ru(Htctpy)-(tfcpbd)(NCS)\{(C_4H_9)_4N\}_2]$ (**3**), are shown in Figure 1.

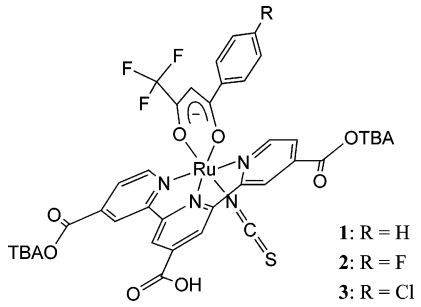

Figure 1. Molecular structures of complexes **1**−**3**. TBA stands for tetrabutylammonium.

Experimental Section

Materials. The following chemicals were purchased and used without further purification: hydrated ruthenium trichloride (from Aldrich), ammonium thiocyanate (from TCI), tetrabutylammonium thiocyanate (from TCI), tetrabutylammonium hydroxide (from Aldrich), 4,4,4-trifluoro-1-(phenyl)butane-1,3-dione (from Aldrich), *tert*-butylpyridine (TBP, from Aldrich). Solvents used in synthesis were of reagent grade. Chromatographic purification was performed by gel permeation on Sephadex LH-20 (from Sigma). 4,4′,4″-Trimethoxycarbonyl-2,2′:6′,2″-terpyridine,[9] 4,4,4-trifluoro-1-(4-chlorophenyl)butane-1,3-dione,[26] 4,4,4-trifluoro-1-(4-fluorophenyl)-butane-1,3-dione,[26] and Ru(4,4′,4″-trimethoxycarbonyl-2,2′:6′,2″-terpyridine)Cl_3[9] were synthesized using literature procedures.

Synthesis of $[Ru(Htctpy)(tfpbd)(NCS)\{(C_4H_9)_4N\}_2]$ (1). To a solution of complex Ru(4,4′,4″-trimethoxycarbonyl-2,2′:6′,2″-terpyridine)Cl_3 (307 mg, 0.5 mmol) in methanol (100 mL) were added tfpbd (430 mg, 2.0 mmol) and Et_3N (0.5 mL). The reaction mixture was refluxed for 8 h, and the solvent was allowed to evaporate on a rotary evaporator. The crude complex Ru(4,4′,4″-trimethoxycarbonyl-2,2′:6′,2″-terpyridine)(tfpbd)Cl was purified on a Sephadex LH-20 column using methanol as eluent. The green band was collected, and the solvent was allowed to evaporate on a rotary evaporator. The solid mass thus obtained was dissolved in 30 mL of DMF under nitrogen. To this solution was added 5 mL of an aqueous solution of NaSCN (300 mg, 3.7 mmol). After the solution was refluxed for 8 h, 10 mL of Et_3N was added and the solution was refluxed for a further 24 h to hydrolyze the ester groups on the terpyridine ligand. The reaction mixture was allowed to cool, and the solvent volume was reduced on a rotary evaporator to about 5 mL. Water was added to the flux, and the insoluble solid was filtered and dried under vacuum. Ru(H_3tctpy)(tfpbd)(NCS) was further purified by loading it onto a Sephadex LH-20 column with water as eluent. Obtained complex Ru(H_3tctpy)(tfpbd)(NCS) (0.1 g) was added to 10 mL of water and dissolved by the addition of a minimum amount of 0.1 M aqueous tetrabutylammonium hydroxide (TBAOH) (the pH of the solution was about 9). To this solution was added 0.1 g of tetrabutylammonium thiocyanate. The resulting solution was filtered to remove a small amount of insoluble material,

(11) Yamaguchi, T.; Yanagida, M.; Katoh, R.; Sugihara, H.; Arakawa, H. *Chem. Lett.* **2004**, *33*, 986.
(12) Islam, A.; Chowdhury, F. A.; Chiba,Y.; Komiya,R.; Fuke, N.; Ikeda, N.; Han, L. *Chem. Lett.* **2005**, *34*, 344.
(13) Renouard, T.; Fallahpour, R.-A.; Nazeeruddin, Md. K.; Humphry-Baker, R.; Gorelsky, S. I.; Lever, A. B. P.; Grätzel, M. *Inorg. Chem.* **2002**, *41*, 367.
(14) Wang, P.; Humphry-Baker, R.; Moser, J. E.; Zakeeruddin, S. M.; Grätzel, M. *Chem. Mater.* **2004**, *16*, 3246.
(15) Nazeeruddin, Md. K.; Zakeeruddin, S. M.; Lagref, J.-J.; Liska, P.; Comte, P.; Barolo, C.; Viscardi, G.; Schenk, K.; Grätzel, M. *Coord. Chem. Rev.* **2004**, *248*, 1317.
(16) Klein, C.; Nazeeruddin, Md. K.; Liska, P.; Censo, D. D.; Hirata, N.; Palomares, E.; Durant, J. R.; Grätzel, M. *Inorg. Chem.* **2005**, *44*, 178.
(17) Wang, P.; Zakeeruddin, S. M.; Moser, J. E.; Humphry-Baker, R.; Comte, P.; Aranyos, V.; Hagfeldt, A.; Nazeeruddin, Md. K.; Grätzel, M. *Adv. Mater.* **2004**, *16*, 1806.
(18) Wang, Z.-S.; Kawauchi, H.; Kashima, T.; Arakawa, H. *Coord. Chem. Rev.* **2004**, *248*, 1381.
(19) Han, L.; Koide, N.; Chiba, Y.; Islam, A.; Komiya, R.; Fuke, N.; Fukui, A.; Yamanaka, R. *Appl. Phys. Lett.* **2005**, *86*, 213501.
(20) Argazzi, R.; Bignozzi, C. A.; Hasselmann, G. M.; Meyer, G. J. *Inorg. Chem.* **1998**, *37*, 4533.
(21) Islam, A.; Sugihara, H.; Hara, K.; Singh, L. P.; Katoh, R.; Yanagida, M.; Takahashi, Y.; Murata, S.; Arakawa, H. *J. Photochem. Photobiol., A* **2001**, *145*, 135.
(22) Yamaguchi, T.; Yanagida, M.; Katoh, R.; Sugihara, H.; Arakawa, H. *Chem. Lett.* **2004**, *33*, 986.
(23) Sugihara, H.; Sano, S.; Yamaguchi, T.; Yanagida, M.; Sato, T.; Abe, Y.; Nagao, Y.; Arakawa, H. *J. Photochem. Photobiol., A* **2004**, *166*, 81.
(24) Takahashi, Y.; Arakawa, H.; Sugihara, H.; Hara, K.; Islam, A.; Katoh, R.; Tachibana, Y.; Yanagida, M. *Inorg. Chim. Acta* **2000**, *310*, 169.
(25) Islam, A.; Sugihara, H.; Yanagida, M.; Hara, K.; Fujihashi, G.; Tachibana, Y.; Katoh, R.; Murata, S.; Arakawa, H. *New J. Chem.* **2002**, *26*, 966.
(26) Sloop, J. C.; Bumgardner, C. L.; Loehle, W. D. *J. Fluorine Chem.* **2002**, *118*, 135.

and the pH was adjusted to 5.0 with dilute hydrochloric acid. A dense precipitate formed immediately, but the suspension was nevertheless refrigerated overnight prior to filtration to collect the product. The flux was allowed to warm to room temperature, and the precipitate was filtered through a sintered glass crucible and dried under vacuum to yield tetrabutylammonium salt [Ru(Htctpy)(tfpbd)(NCS){$(C_4H_9)_4N$}$_2$] (**1**). Yield: 45%. ^{1}H NMR (300 MHz, DMSO): δ 9.29 (H, s), 9.23 (3H, ss), 8.72 (H, d), 8.65 (H, d), 8.37 (H, d), 8.15 (H, d), 8.09 (H, d), 7.75 (H, d), 7.69 (H, m), 7.22 (H, m), 7.05 (H, m), 6.52 (0.5H, s), 6.46 (0.5H, s), 3.16 (16H, t), 1.56 (16H, m), 1.31 (16H, m), 1.01 (24H, t). Anal. Calcd for $C_{61}H_{87}F_3N_6O_8RuS$: C, 59.93; H, 7.17; N, 6.87. Found: C, 59.12; H, 7.25; N, 6.52.

Synthesis of [Ru(Htctpy)(tffpbd)(NCS){$(C_4H_9)_4N$}$_2$] (2). Using the same conditions as for complex **1** and starting from ligand 4,4,4-trifluoro-1-(4-fluorophenyl)butane-1,3-dione, we obtained the title compound, [Ru(Htctpy)(tffpbd)(NCS){$(C_4H_9)_4N$}$_2$] (**2**), as a dark green powder. Yield: 35%. ^{1}H NMR (300 MHz, DMSO): δ 9.16 (4H, ss), 8.77 (H, d), 8.72 (H, d), 8.46 (H, m), 8.21 (H, d), 8.15 (H, d), 7.51 (H, m), 7.32 (H, m), 6.97 (H, t), 6.53 (0.5H, s), 6.49 (0.5H, s), 3.26 (16H, t) 1.64 (16H, m), 1.41 (16H, m), 1.02 (24H, t). Anal. Calcd for $C_{61}H_{86}F_4N_6O_8RuS$: C, 59.06; H, 6.99; N, 6.77. Found: C, 58.89; H, 6.79; N, 6.61.

Synthesis of [Ru(Htctpy)(tfcpbd)(NCS){$(C_4H_9)_4N$}$_2$] (3). Using the same conditions as for complex **1** and starting from ligand 4,4,4-trifluoro-1-(4-chlorophenyl)butane-1,3-dione, we obtained the title compound, [Ru(Htctpy)(tfcpbd)(NCS){$(C_4H_9)_4N$}$_2$] (**3**), as a dark green powder. Yield: 45% as a dark green powder. ^{1}H NMR (300 MHz, DMSO): δ 9.15 (4H, ss), 8.77 (H, d), 8.72 (H, d), 8.37 (H, d), 8.20 (H, d), 8.11 (H, d), 7.73 (H, d), 7.25 (2H, q), 6.54 (0.5H, s), 6.50 (0.5H, s), 3.20 (16H, t) 1.54 (16H, m), 1.37 (16H, m), 1.01 (24H, t). Anal. Calcd for $C_{61}H_{86}ClF_3N_6O_8RuS$: C, 58.29; H, 6.90; N, 6.69. Found: C, 58.12; H, 6.95; N, 6.75

Spectroscopic Measurements. UV−visible spectra were recorded on a Shimadzu UV-3101PC spectrophotometer. Steady-state emission spectra were recorded using a grating monochromator (Triax 1900) with a CCD image sensor. The spectral sensitivity of the spectrophotometer was corrected using a bromine lamp (Ushio IPD100V 500WCS). A sample in a 3 mm quartz round cell was excited using an Nd^{3+}:YVO4 laser (CASIX, 532 nm, CW 30 mW). A Dewar vessel was used for the measurements at 77 K. Emission lifetimes were measured using a time-correlated single photon counting (TCSPC) system. The second harmonic (400 nm, 10 kHz to 2 MHz repetition rate) of a laboratory-made femtosecond Ti^{3+}: sapphire laser with a cavity dumper was used for excitation of a sample in a 3 mm quartz cell. The TCSPC data were analyzed using the convolution method with an instrumental response function (IRF, 35 ps). ^{1}H NMR spectra were recorded with a Varian 300BB spectrometer. ATR-FTIR spectra were measured at 2 cm^{-2} resolution and averaged over 80 scans. Measurements were made with the same mechanical force used to push the samples into contact with the diamond window. The FTIR spectra of the anchored dyes were obtained by subtracting the IR spectrum of blank TiO_2 films from the IR spectrum of dye-coated TiO_2 films of the same thickness.

Electrochemical Measurements. The redox potential of the complexes was measured using a standard three-electrode apparatus. The counter electrode was a platinum wire, the working electrode a ruthenium-complex-adsorbed conducting nanocrystalline TiO_2 film, and the reference electrode a Ag/AgCl (saturated aqueous KCl) in contact with a KCl salt bridge. Cyclic voltammograms were collected using an electrochemical analyzer. Scan rates were 0.05−0.5 V s^{-1}. Acetonitrile was used as solvent and the supporting electrolyte was 0.1 M tetrabutylammonium perchlorate. Electrode potential values were corrected to the saturated calomel electrode (SCE).

Computation Methods. The geometry of complex **2** in the ground state was calculated via density functional theory using the TURBOMOLE 5.7 program package.[27] The resolution of the identity approximation using the RI-J auxiliary basis[28] was employed for efficient treatment of Coulomb interactions in the DFT calculation with a BP86 pure density functional.[29] The excitation energies and oscillator strengths were calculated via time-dependent density functional theory (TD-DFT) using the Gaussian 98, rev A11.3 suite.[30] A Beck's style three-parameter hybrid functional with a correlation function of PW91 (B3PW91) was employed with the basis functions of Dunning−Hay's split valence double-ζ for C, H, N, and O atoms (D95) and Hay−Wadt double-ζ with Ros Alamos relativistic effective core potential for ruthenium atoms (LANL2DZ). Molecular orbitals were visualized with the population analysis at the B3PW91/LANL2DZ level using the Molekel program.[31−32]

Preparation of TiO_2 Electrode. Nanocrystalline TiO_2 photoelectrodes of about 20 μm thickness (area: 0.25 cm^2) were prepared using a variation of a method reported by Graetzel and co-workers.[9] Fluorine-doped tin oxide-coated glass electrodes (Nippon Sheet Glass Co., Japan) with a sheet resistance of 8−10 ohm^{-2} and an optical transmission of greater than 80% in the visible range were used. Anatase TiO_2 colloids (particle size ~13 nm) were obtained from commercial sources (Ti-Nanoxide D/SP, Solaronix). The nanocrystalline TiO_2 thin films of approximately 20 μm thickness were deposited onto the conducting glass by screen-printing. The film was then sintered at 500 °C for 1 h. The film thickness was measured with a Surfcom 1400A surface profiler (Tokyo Seimitsu Co. Ltd.). The electrodes were impregnated with a 0.05 M titanium tetrachloride solution and sintered at 500 °C. The dye solutions (2×10^{-4} M) were prepared in 1:1 acetonitrile and *tert*-butyl alcohol solvents. Deoxycholic acid was added to the dye solution as a coadsorbent at a concentration of 20 mM. The electrodes were immersed in the dye solutions and then kept at 25 °C for 20 h to adsorb the dye onto the TiO_2 surface.

Fabrication of Dye-Sensitized Solar Cell. Photovoltaic measurements were performed in a two-electrode sandwich cell configuration. The dye-deposited TiO_2 film was used as the working electrode and a platinum-coated conducting glass as the counter-electrode. The two electrodes were separated by a Surlyn spacer (50 um thick) and sealed up by heating the polymer frame. The electrolyte was composed of 0.6 M dimethylpropyl-imidazolium

(27) Ahlrichs, R.; Bär, M.; Häser, M.; Horn, H.; Kölmel, C. *Chem. Phys. Lett.* **1989**, *165*, 162.
(28) Eichkorn, K.; Weigend, F.; Treutler, O.; Ahlrichs, R. *Theor. Chem. Acc.* **1997**, *119*, 97.
(29) te Velde, G.; Baerends, J. *Comput. Phys.* **1992**, *99*, 84.
(30) Frisch, M. J.; Trucks, G. W.; Schlegel, H. B.; Scuseria, G. E.; Robb, M. A.; Cheeseman, J. R.; Zakrzewski, V. G.; Montgomery, J. A.; Stratmann, R. E.; Burant, J. C.; Dapprich, S.; Millam, J. M.; Daniels, A. D.; Kudin, K. N.; Strain, M. C.; Farkas, O.; Tomasi, J.; Barone, V.; Cossi, M.; Cammi, R.; Mennucci, B.; Pomelli, C.; Adamo, C.; Clifford, S.; Ochterski, J.; Petersson, G. A.; Ayala, P. Y.; Cui, Q.; Morokuma, K.; Malick, D. K.; Rabuck, A. D.; Raghavachari, K.; Foresman, J. B.; Cioslowski, J.; Ortiz, J. V.; Stefanov, B. B.; Liu, G.; Liashenko, A.; Piskorz, P.; Komaromi, I.; Gomperts, R.; Martin, R.L.; Fox, D. J.; Keith, T.; Al-Laham, M. A.; Peng, C. Y.; Nanayakkara,A.; Gonzalez, C.; Challacombe, M.; Gill, P. M. W.; Johnson, B. G.; Chen, W.; Wong, M. W.; Andres, J. L.; Head-Gordon, M.; Replogle, E. S.; Pople, J. A. *Gaussian 98*, revision A.11.3; Gaussian Inc.: Pittsburgh, PA, 1998.
(31) Flukiger, P.; Luthi, H. P.; Portmann, S.; Weber, J. *Molekel*, version 4.3; Swiss Center for Scientific Computing: Manno, Switzerland, 2000−2002.
(32) Portmann, S.; Luthi, H. P. *MOLEKEL: An Interactive Molecular Graphics Tool*; *Chimia* **2000**, *54*, 766.

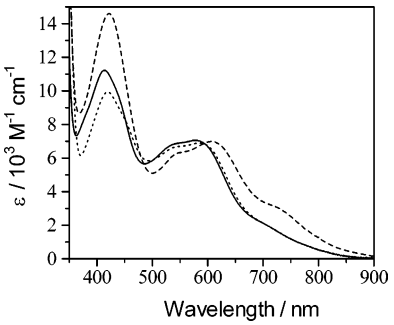

Figure 2. UV−vis absorption spectra of complex **1** (...), complex **2** (—), and [Ru(4,4′,4″-tricarboxy-2,2′:6′,2″-terpyridine)(1,1,1-trifluoropentane-2,4-dionato)(NCS)] (− − −) in a 4:1 ethanol:methanol solution.

iodide (DMPII), 0.05 M I_2, and 0.1 M LiI in acetonitrile (AN) with or without *tert*-butylpyridine (TBP).

Photovoltaic Characterization. The working electrode was illuminated through a conducting glass. The current−voltage characteristics were measured using the previously reported method[33] with a solar simulator (AM-1.5, 100 mW/cm^2, WXS-155S-10: Wacom Denso Co. Japan). Monochromatic incident photon-to-current conversion efficiency (IPCE) for the solar cell, plotted as a function of excitation wavelength, was recorded on a CEP-2000 system (Bunkoh-Keiki Co. Ltd.). Incident photon-to-current conversion efficiency (IPCE) at each incident wavelength was calculated from eq 1, where I_{sc} is the photocurrent density at short circuit in mA cm^{-2} under monochromatic irradiation, q is the elementary charge, λ is the wavelength of incident radiation in nm, and P_0 is the incident radiative flux in W m^{-2}.

$$\mathrm{IPCE}(\lambda) = 1240(I_{sc}/q\lambda P_0) \quad (1)$$

Results and Discussion

UV−visible absorption. The absorption spectra of the aryl-substituted β-diketonato-ruthenium(II)-polypyridyl complexes **1** and **2** in ethanol−methanol solution are shown in Figure 2 together with that of the [Ru(4,4′,4′′-tricarboxy-2,2′:6′,2′′-terpyridine)(1,1,1-trifluoropentane-2,4-dionato)-(NCS)] (**C1**) complex for comparison. The spectrochemical and electroch.emical properties of complexes **1**−**3** and **C1** are summarized in Table 1. The diketonate ruthenium(II) complexes **1**−**3** and **C1** all show intense UV bands between 290 and 329 nm and are assigned to the intraligand $\pi-\pi^*$ transition of the 4,4′,4″-tricarboxy-2,2′:6′,2″-terpyridine ligand.[34] Intense and broad metal-to-ligand charge transfer (MLCT) bands of complexes **1**−**3** are observed in the visible region between 413 and 589 nm. In complexes **1**−**3**, the molar extinction coefficient of the lowest energy MLCT band shows in the range of 6200−7000 M^{-1} cm^{-1}.[34] The lower-energy MLCT band maximum of complex **1** is observed at 589 nm, which is blue-shifted by about 17 nm compared to that of complex **C1**. Substitution of the methyl group of the 1,1,1-trifluoropentane-2,4-dionato ligand with the phenyl group in complex **1** stabilizes the ground state by electron withdrawal from Ru, causing a decrease in the energy of the t_{2g} metal orbital compared to that of complex **C1** and thus blue-shifts the lowest-energy MLCT band. When compared to the 4,4,4-trifluoro-1-(phenyl)butane-1,3-dione complex **1**, which shows a maximum at 589 nm, the lowest MLCT band of complex **2** is blue-shifted (from 589 to 586 nm) because of the stronger electron-withdrawing nature of the fluorine-substituted aryl group present in the 4,4,4-trifluoro-1-(4-fluorophenyl)butane-1,3-dione ligands of complex **2**. In the red-light region, the diketonato complexes **1**−**3** all show a distinct shoulder at around 680 nm, which is assigned to metal-to-ligand charge transfer (MLCT) transition (Figure 2).[24] The enhanced red absorption of these complexes renders them attractive candidates as panchromatic charge-transfer sensitizers for DSCs. Figure 3 compares the absorption spectra of complex **2** adsorbed on TiO_2 thin film and in ethanol−methanol solution. The two spectra are similar, but the absorption bands of the dye on the TiO_2 electrode are broader and slightly red-shifted compared to the absorption spectrum in solution. This peak energy shift, observed in many Ru-based complexes,[2,12,24,35] may be due to a change in their energy levels in the ground and excited states compared to in the solution state resulting from interaction between the dye and the electrode. This broadening of the absorption spectrum is desirable for harvesting the solar spectrum and leads to a large photocurrent.

Emission Spectra. It is well-known that the excited-state responsible for the luminescence of the Ru(II)−polypyridine compounds is the lowest-energy triplet metal-to-ligand charge-transfer (^{3}MLCT) state.[36] When excited at the charge-transfer absorption band, complexes **1**−**3** show an intense and structured emission at the 77 K ethanol−methanol glass matrix with a maximum between 835 and 841 nm. In degassed ethanol−methanol solution at 298 K, the emission spectra become weak and broad with a small shift to the lower-energy end. The blue shift that occurs for all of the complexes in the transition from fluid solution to frozen solvent glass is a common rigidochromic effect observed in many metal diamine complexes.[36−37] The emission spectra of complex **2** in ethanol−methanol mixed solvents at 77 and 298 K are presented in Figure 4. The luminescence data are gathered in Table 1. At 77 K, complexes **1**−**3** displayed excited-state lifetimes ranging from 338 to 370 ns. The lifetimes decreased significantly with increasing temperature, to 8−13 ns in fluid solution at 298 K. The very short-lived excited-state in fluid solution may be caused by efficient nonradiative decay via low-lying ligand-field excited states.[36] The excited-state lifetime (8−13 ns) of all the complexes is long enough for the process of electron injection into the conduction band of the TiO_2 electrode to be efficient, as the injection process occurs on a time scale of femtoseconds or picoseconds.[38−39]

DFT Calculations. Results from a density functional theory (DFT) calculation of complex **2** are presented in Figure 5, showing the Frontier molecular orbital (MOs)

(33) Koide, N.; Han, L. *Rev. Sci. Instrum.* **2004**, *75*, 2828.
(34) Mamo, A.; Juris, A.; Calogero, G.; Campagna, S. *Chem. Commun.* **1996**, *1225*.
(35) Islam, A.; Hara, K.; Singh, L.P.; Katoh, R.; Yanagida, M.; Murata, S.; Takahashi, Y.; Sugihara, H.; Arakawa, H. *Chem. Lett.* **2000**, 490.
(36) Islam, A.; Ikeda, N.; Yoshimura, A.; Ohno, T. *Inorg. Chem.* **1998**, *37*, 3093.
(37) Juris, A.; Balzani, V.; Barigelletti, F.; Campagna, S.; Belser, P.; Zelewsky, A. *Coord. Chem. Rev.* **1988**, *84*, 85.
(38) Tachibana, Y.; Haque, S. A.; Mercer, I. P.; Durrant, J. R.; Klug, D. R. *J. Phys. Chem. B* **2000**, *104*, 1198.
(39) Rehm, J. M.; McLendon, G. L.; Nagasawa, Y.; Yoshihara, K.; Moser, J.; Graetzel, M. *J. Phys. Chem.* **1996**, *100*, 9577.

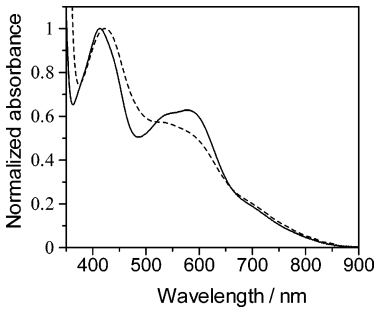

Figure 3. UV−vis absorption spectra of complex **2** in a 4:1 ethanol:methanol solution (—) and adsorbed onto a nanocrystalline 7 μm thick TiO_2 film (− − −).

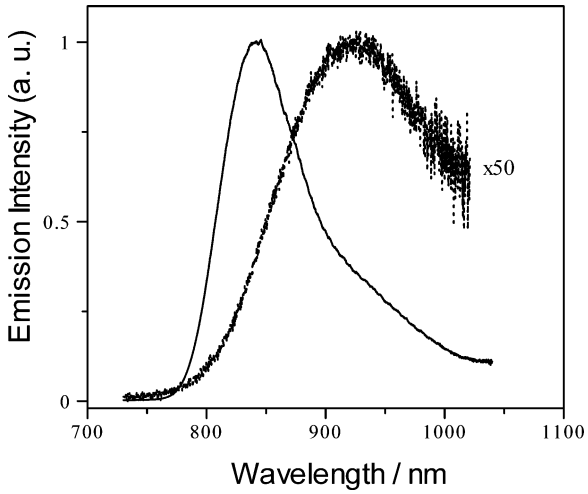

Figure 4. Corrected emission spectra of complex **2** in a 4:1 ethanol:methanol solution at 77 K (—) and 298 K (···).

surfaces. The energy levels of MOs and their parentages are summarized in Table 2. The LUMO is mainly the π^* 4,4′,4″-tricarboxy-2,2′:6′,2″-terpyridine ligand with a considerable amount of π back-donation from the t_{2g} orbital. The LUMO has sizable contributions from the carboxylic groups, enhancing electronic coupling to the TiO_2 conduction band states. The HOMO in Figure 5 is formed from an antibonding interaction between the t_{2g} orbital of ruthenium and the π-orbital of NCS. The NCS group pointing in the direction of the electrolyte may facilitate reduction of the oxidized dye (Ru^{3+}) through reaction with I^-, making it particularly suitable for highly efficient solar cells. The π-orbitals on the β-diketonato ligand have a negligible contribution to HOMO. Only the NCS donor ligand of the studied complexes 1−3 is thus an active participant in dye regeneration via interaction with the I^-.

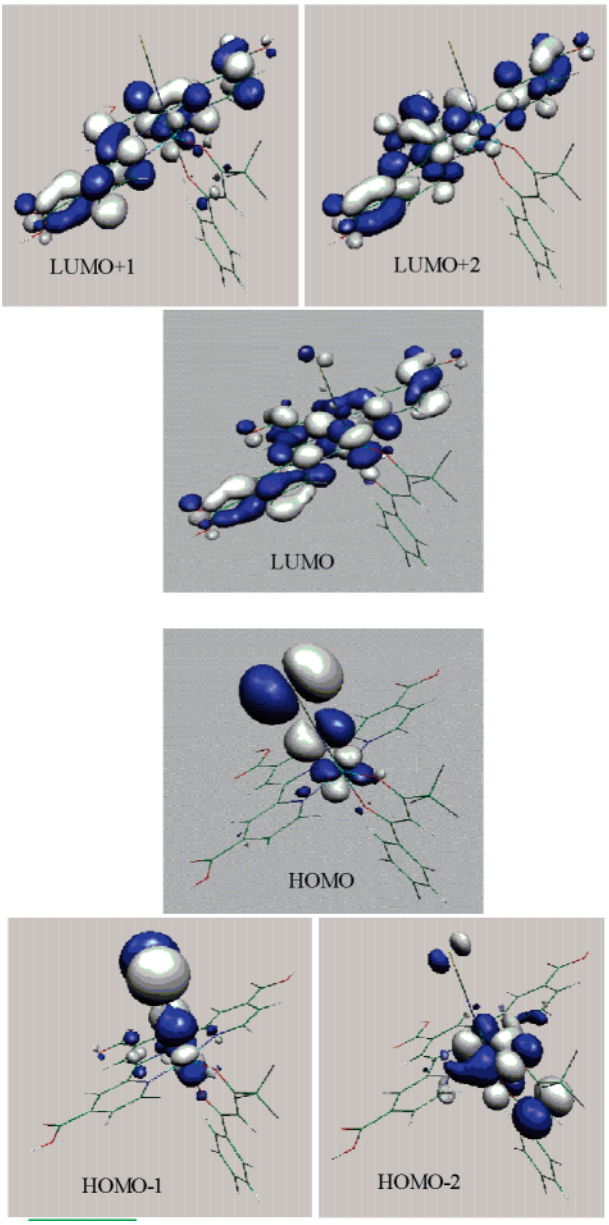

Figure 5. Frontier MOs as obtained in this work for complex **2**.

Electrochemical Data. The electrochemical properties of complexes **1**−**3** and **C1** adsorbed onto TiO_2 (6 μm) were investigated in 0.1 M $LiClO_4$ acetonitrile solution by cyclic voltammetry. The data are given in Table 1. Typical cyclic voltammograms for complexes **1** and **2** on TiO_2 are shown in Figure 6. All the complexes exhibit a quasi-reversible

Table 1. Absorption, Luminescence, and Electrochemical Properties of the Ruthenium Complexes

sensitizer	absorption,[a] λ_{max} (nm) (ϵ ($\times 10^3$ $M^{-1}cm^{-1}$))	emission λ_{max}[b] (nm) 298 K	emission λ_{max}[b] (nm) 77 K	emission τ[b] (ns) 298 K	emission τ[b] (ns) 77 K	E ($Ru^{3+/2+}$)[c] vs SCE	E^* ($Ru^{3+/2+}$)[d] vs SCE
1	290 (27.6), 320 (22.9), 420 (9.9), 589 (6.9)	920	837	10	368	+0.72	−0.85
2	290 (27.8), 319 (23.2), 413 (11.2), 586 (7.0)	915	835	13	370	+0.73	−0.86
3	290 (27.7), 322 (25.5), 414 (8.9), 584 (6.2)	920	841	8	338	+0.72	−0.87
C1[e]	293 (27.6), 331 (22.7), 422 (14.6), 606 (7.0)	940		16		+0.68[f]	

[a] Measured in 4:1 v/v ethanol:methanol at room temperature. [b] The emission spectra and emission lifetime were obtained by exciting into the lowest MLCT band in 4:1 v/v ethanol:methanol. [c] Half-wave potentials assigned to the $Ru^{3+/2+}$ couple for ruthenium sensitizers bound to nanocrystalline TiO_2 film, measured in 0.1 M $LiClO_4$ acetonitrile solution. [d] Calculated from E^* ($Ru^{3+/2+}$) = E ($Ru^{3+/2+}$) − E^{0-0}; E^{0-0} values were estimated from the 5% intensity level of the emission spectra at 77 K. [e] Data taken from ref 25. [f] Measured after adsorption onto TiO_2 film.

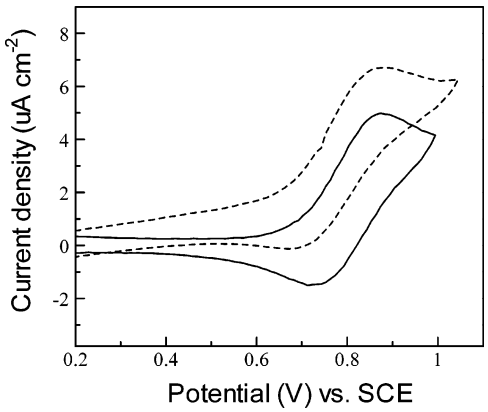

Figure 6. Cyclic voltammograms of complexes **2** (—) and **3** (– – –) adsorbed on nanocrystalline TiO_2 electrodes in 0.1 M $LiClO_4$ acetonitrile solution.

Table 2. Energy Levels of Frontier MOs and Their Parentages for Complex 2

molecular orbital	energy (eV)	major contribution
LUMO+4	−2.333	π^*(tctpy)
LUMO+3	−2.429	π^*(tffpbd)
LUMO+2	−2.579	π^*(tctpy)
LUMO+1	−2.869	(π^*(tctpy)−Ru(t_{2g}))*
LUMO	−3.227	(π^*(tctpy)−Ru(t_{2g}))*
HOMO	−5.239	(Ru(t_{2g})− π(NCS))*
HOMO-1	−5.240	(Ru(t_{2g})− π(NCS))*
HOMO-2	−6.519	(Ru(t_{2g})−π(tffpbd))*
HOMO-3	−6.804	(Ru(t_{2g})−π(NCS))
HOMO-4	−6.961	(Ru(t_{2g})−π(NCS))

oxidation wave for the $Ru^{3+/2+}$ couple ranging from +0.72 to +0.73 V vs SCE. Table 1 shows that the ground-state oxidation potentials ($Ru^{3+/2+}$) of the β-diketonato complexes **1**−**3** are more positive than those of the complex **C1**. For complexes **1**−**3** and **C1**, the energy of the acceptor orbital (LUMO) remains nearly constant and the increase in the MLCT transition energy of complexes **1**−**3** arises mainly from the decrease in the energy of MOs containing the metal t_{2g} orbital. The energy difference between the $Ru^{3+/2+}$ potential of complexes **1**−**3** and the I_3^-/I^- redox couple (0.07 V vs SCE)[40] is large enough for efficient regeneration of Ru(II) through reaction with iodide. The excited-state oxidation potential, E^* ($Ru^{3+/2+}$), is a measure of the loss of the electron that is placed in the π^* (terpyridine) LUMO upon excitation. For complexes **1**−**3**, E^* ($Ru^{3+/2+}$) values are estimated using eq 2, where E ($Ru^{3+/2+}$) is the oxidation potential of the ground state and E^{0-0} is the energy difference between the lowest excited and ground states. The resulting E^* ($Ru^{3+/2+}$) values are shown in Table 1. The excited states of complexes **1**−**3** lie above the conduction band edge (−0.82 V vs SCE) of the nanocrystalline TiO_2.[6] Efficient electron injection into the conduction band of the TiO_2 is therefore expected to be possible with all of complexes **1**−**3**.

$$E^*(Ru^{3+/2+}) = E^*(Ru^{3+/2+}) - E^{0-0} \quad (2)$$

ATR-FTIR Spectral Data. Figure 7 shows ATR-FTIR spectra of complexes **1** and **2** measured as a solid and in the form adsorbed onto TiO_2 films. The studied complexes **1**−**3** all contain one carboxylic acid and two carboxylate groups

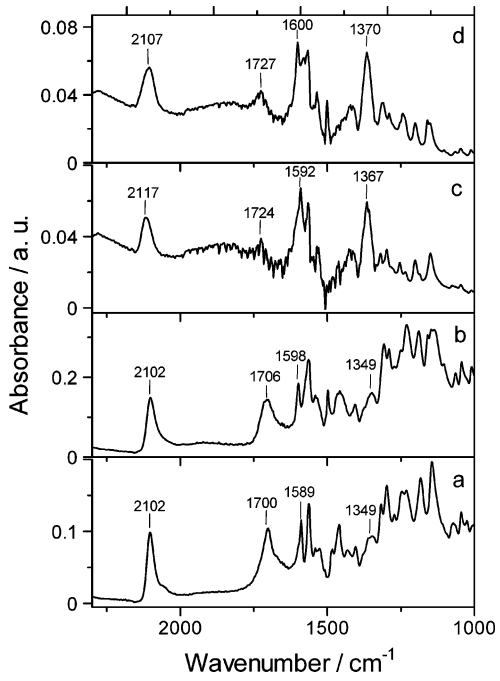

Figure 7. ATR-FTIR spectra of complexes **1** and **2** obtained using powder samples and adsorbed on the 7 μm thick TiO_2 films: (a) complex **1** powder; (b) complex **2** powder; (c) complex **1** adsorbed on TiO_2 film; and (d) complex **2** adsorbed on TiO_2 film.

(see Figure 1). The ATR-FTIR spectra of complexes **1** and **2** show bands due to asymmetric and symmetric carboxylate groups at 1589−1598 cm^{-1} (COO^-_{as}) and 1349 cm^{-1} (COO^-_s), respectively (panels a and b of Figure 7).[41] A band due to the υ(−C═O) of the carboxylic acid group was observed at 1700 and 1706 cm^{-1} in complexes **1** and **2**, respectively. Both complexes show a broadband at 2102 cm^{-1} due to the υ(NC) of the thiocyanate ligand. The ATR-FTIR spectra of complexes **1** and **2** adsorbed onto TiO_2 film show a marked increase in the intensity of asymmetric (1592−1600 cm^{-1}; COO^-_{as}) and symmetric (1367−1370 cm^{-1}; COO^-_s) carboxylate bands compared with the corresponding peaks of the powder (panels c and d of Figure 7) together with a strong υ(NC) of the thiocyanate group at 2107−2117 cm^{-1}. The intense band at around 1700−1706 cm^{-1} for the carboxylic acid mode of complexes **1** and **2** nearly disappears after grafting onto the TiO_2 surface. These indicate that the carboxylic acid is dissociated to the carboxylate group on the TiO_2 surface and implicated in the surface attachment of the dye.

Photovoltaic Properties. The photovoltaic performance of complexes **1**−**3** on nanocrystalline TiO_2 electrode was studied under standard AM 1.5 irradiation (100 mW cm^{-2}) using an electrolyte with a composition of 0.6 M dimethylpropyl-imidazolium iodide (DMPII), 0.05 M I_2, and 0.1 M LiI in acetonitrile. The short-circuit photocurrent density (J_{sc}), open-circuit voltage (V_{oc}), fill factors (FF) and overall cell efficiencies (η) for each dye-TiO_2 electrode are summarized in Table 3. Figure 8 shows the photocurrent action spectra for the cells with complexes **1** or **2** where the incident photon to current conversion efficiency (IPCE) values are plotted

(40) Oskam, G.; Bergeron, B. V.; Meyer, G. J.; Searson, P. C. *J. Phys. Chem. B* **2001**, *105*, 6867.

(41) Nazeeruddin, Md. K.; Humphry-Baker, R.; Liska, P.; Grätzel, M. *J. Phys. Chem. B* **2003**, *107*, 8981.

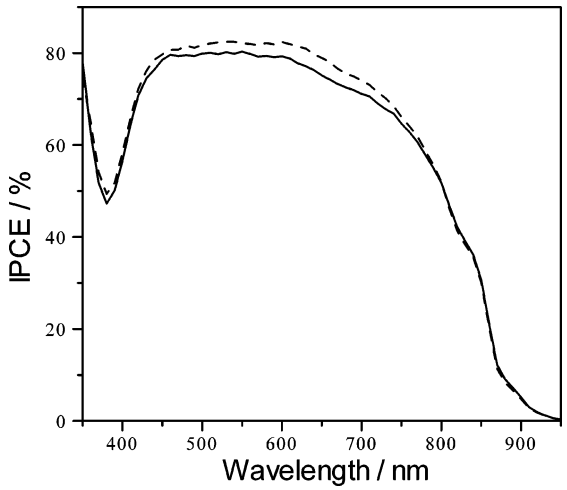

Figure 8. Photocurrent action spectra obtained with complexes **1** (– – –) and **2** (—) attached to nanocrystalline TiO_2 film. The incident photon-to-current conversion efficiency is plotted as a function of wavelength. A sandwich type sealed cell configuration was used to measure this spectrum. The electrolyte composition was 0.6 M DMPII, 0.1 M I_2, and 0.1 M LiI in acetonitrile.

Table 3. Photovoltaic Properties of Ruthenium Dye-Sensitized TiO_2 Solar Cells[a]

sensitizer	$IPCE_{max}$ (%)	J_{sc} (mA cm^{-2})	V_{oc} (V)	FF	η (%)
1	80	22.4	0.58	0.67	8.7
2	78	22.0	0.59	0.68	8.8
3	75	20.9	0.55	0.67	7.7
C1	70[b]	18.3[b]	0.57	0.64	6.7

[a] Conditions: sealed cells; coadsorbate, DCA 40 mM; photoelectrode, TiO_2 (25 μm thickness and 0.25 cm^2); electrolyte, 0.6 M DMPII, 0.1 M LiI, 0.05 I_2 in AN; irradiated light, AM 1.5 solar light (100mW cm^{-2}). J_{sc}, short-circuit photocurrent density; V_{oc}, open-circuit photovoltage; FF, fill factor; η, total power conversion efficiency; IPCE, incident photon-to-current conversion efficiency. [b] Data taken from ref 25.

as a function of wavelength. The maximum IPCE values of complexes **1**−**3** at the lowest-energy MLCT band are given in Table 3. All the complexes show better cell performance compared to complex **C1** and this improvement may be due to the increase in the dye regeneration rate after tuning the ground-state oxidation potential to more positive value.

All the complexes achieved efficient sensitization of nanocrystalline TiO_2 over the whole visible range extending into the near IR region (ca. 950 nm). The most efficient sensitizers in the series were complexes **1** and **2**, with an IPCE value of 80% in the plateau region. Taking into account the reflection and absorption losses by the conducting glass, the efficiency of electric current generation in this range reaches about 90% over a broad wavelength range extending from 450 to 620 nm.

Of the three new complexes synthesized, 4,4,4-trifluoro-1-(4-fluorophenyl)butane-1,3-dione (complex **2**) presents the best photovoltaic results, with an overall conversion efficiency (η) of 8.8%. The photovoltaic performance parameters of complex **2**-sensitized cells were studied using electrolytes with various TBP concentrations. The short-circuit photocurrent decreased as the TBP concentrations increased. In contrast, the open-circuit voltage increased significantly at a TBP concentration of 0.07 M, and the fill factor increased slightly. TBP probably adsorbed on the bare TiO_2 surface and suppress the recombination between the injected electrons and I_3^- ions.[2,42] Figure 9 shows photocurrent voltage curves of a sandwich-type sealed solar cell based on complex **2** at standard AM 1.5 irradiation with different incident light intensities and under dark conditions using an electrolyte of 0.6 M dimethylpropyl-imidazolium iodide (DMPII), 0.05 M I_2, 0.1 M LiI, and 0.07M tert-butylpyridine (TBP) in acetonitrile. As shown in Table 4, the solar cell sensitized with complex **2** showed a photocurrent density of 19.1 mA cm^{-2}, an open circuit potential of 0.66 V, and a fill factor of 0.72, corresponding to an overall conversion efficiency (η) of 9.1% with the electrolyte containing 0.07 M TBP under standard AM 1.5 irradiation (100 mW cm^{-2}). The overall conversion efficiency remains unchanged at lower incident light intensities. Thus, this class of aryl-substituted compounds serves as a basis for further design of new potential sensitizers by introducing suitable substituents on the phenyl ring to enhance the molar extinction coefficient of the sensitizer and, furthermore, to prevent surface aggregation of the sensitizer.[25]

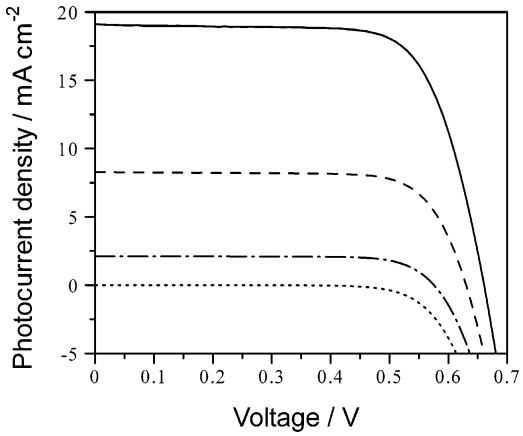

Figure 9. Photocurrent voltage characteristics of DSCs sensitized with the complex **2** at AM 1.5 illuminations (light intensities: (—) 100 mW cm^{-2}; (– – –) 42.8 mW cm^{-2}; (-•-•-) 10.1 mW cm^{-2}) and in the dark (•••). The redox electrolyte consisted of a solution of 0.6 M DMPII, 0.1 M I_2, 0.1 M LiI, and 0.07 M TBP in acetonitrile.

Table 4. Detailed Photovoltaic Parameters of DSCs with Complex 2 Under Different Incident Light Intensities[a]

P_{in} (mW cm^{-2})	J_{sc} (mA cm^{-2})	V_{oc} (mV)	FF	P_{max} (mW cm^{-2})	η (%)
100	19.10	661	0.722	9.12	9.12
42.8	8.30	630	0.748	3.91	9.14
10.1	2.11	576	0.763	0.93	9.18

[a] Conditions: sealed cells; dye, **2**; coadsorbate, DCA 40 mM; photoelectrode, TiO_2 (20 μm thickness and 0.25 cm^2); electrolyte, 0.6 M DMPII, 0.1 M LiI, 0.05 I_2, 0.07 M TBP in AN; irradiated light, AM 1.5 solar light. P_{in}, incident power intensity; J_{sc}, short-circuit photocurrent density; V_{oc}, open-circuit photovoltage; P_{max}, maximum electricity output power density; FF, fill factor;η, total power conversion efficiency.

Conclusions

We succeeded in developing a series of novel panchromatic photosensitizers based on 4,4′,4″-tricarboxy-2,2′:6′,2″-terpyridine-ruthenium(II) complexes with one aryl-substituted β-diketonato chelating ligand, 4,4,4-trifluoro-1-(phenyl)-butane-1,3-dione, 4,4,4-trifluoro-1-(4-chlorophenyl)butane-1,3-dione, or 4,4,4-trifluoro-1-(4-fluorophenyl)butane-1,3-

(42) Hara, K.; Dan-oh, Y.; Kasada, C.; Ohga, Y.; Shinpo, A.; Suga, S.; Sayama, K.; Arakawa, H. *Langmuir* **2004**, *20*, 4205.

dione, and systematically characterized the series using electrochemical and spectroscopic methods. The complexes achieved very efficient sensitization of nanocrystalline TiO_2 over the whole visible range extending into the near IR region (ca. 950 nm). The photovoltaic data of these new complexes show 9.1% power conversion efficiency under standard AM 1.5 irradiation (100 mW cm^{-2}). Further study will target the development of a high-performance solar cell through modification of the electronic and steric environments of the sensitizers on the basis of alteration of the substituents on the β-diketonato ligand.

Acknowledgment. We thank Dr. Hideki Sugihara and Dr. Masatoshi Yanagida (AIST, Tsukuba, Japan) for their helpful discussions. K.N. gratefully acknowledges the Ministry of Education, Science, Sports, and Culture for a Grant-in-Aid for Scientific Research (16550056).

CM0602141